Lc 3 1176 00060 2632

TECHNICAL NOTES

NATIONAL ADVISORY COMMITTEE FOR AERONAUTICS

Copy 1

---

No. 601

---

# THE LATERAL INSTABILITY OF DEEP RECTANGULAR BEAMS

By C. Dumont and H. N. Hill
Aluminum Company of America

---

Washington
May 1937

NATIONAL ADVISORY COMMITTEE FOR AERONAUTICS

# E R R A T A

TECHNICAL NOTE NO. 601

THE LATERAL INSTABILITY OF DEEP RECTANGULAR BEAMS

Page 21, seventh line from bottom: "w (lb. per sq. in.)" should read "w (lb. per in.)".

Page 23, final equation: "$wL_{CR} = 6.11 \sqrt{\frac{EI_z GJ}{L^2}}$" should read

"$wL_{CR} = 6.11 \frac{\sqrt{EI_z GJ}}{L^2}$".

Figure 12: "W per foot" should read "w (lb. per in.)".

NATIONAL ADVISORY COMMITTEE FOR AERONAUTICS

TECHNICAL NOTE NO. 601

# THE LATERAL INSTABILITY OF DEEP RECTANGULAR BEAMS

By C. Dumont and H. N. Hill

## SUMMARY

Experimental and analytical studies were made of solid and hollow deep rectangular beams to study their lateral instability under various conditions of loading and restraint. The tests were made on bars and tubes of 17ST aluminum alloy. Failure by lateral buckling occurred only in tests on the solid beams. It was found that, within the elastic range, the test results were in agreement with the classical theory for the lateral buckling of deep beams as given by Prandtl, Michell, and Timoshenko. The tests were extended to the inelastic range where it was found that the substitution for Young's modulus of an average modulus of elasticity derived from the stress-strain curve made it possible to predict instability at high stresses.

## INTRODUCTION

Rectangular bars are occasionally used in the form of beams with the long dimension of the rectangle in the plane of the loads. When the depth of such a beam is great compared with the width, the beam may become unstable in a lateral direction with a consequent sidewise buckling, perhaps at a stress below the yield strength of the material. This action is similar to the buckling of a column under an axial load. In the lateral buckling of beams, however, the stability depends on the torsional as well as the flexural stiffness. A consideration of stability is frequently of greater importance in designing with aluminum alloys than it is with other structural materials having higher moduli of elasticity. It seems desirable to include in the Handbook, "Structural Aluminum," a section on lateral stability of beams. In order to arrive at a suitable formula for allowable working stresses, it is necessary to have an understanding of the factors contributing to the lateral stability of such a beam, and the effect of different conditions of loading and restraint.

The problem of the lateral instability of deep rectangular beams appears to have been treated first by Prandtl (reference 1) in 1899. In the same year the problem was discussed by A. G. M. Michell (reference 2). Both investigators arrived at substantially the same solution. The subject was further discussed by S. Timoshenko (reference 3), who treated various conditions of loading and lateral restraint. More recently, treatments of the problem have appeared in various textbooks. (See reference 4, p. 609; reference 5, p. 499; reference 6, p. 239.)

That the resulting expression for allowable working stresses may be applied generally with safety, but without being unnecessarily conservative, it is necessary to study the stability of deep rectangular beams under different types of loading and with various conditions of restraint. The solution of the stability problem for certain cases is available from the literature on the subject. For other conditions of loading and support considered, it has been necessary to determine analytically the expressions for the critical loads.

The available literature on the lateral stability of deep rectangular beams deals exclusively with the theoretical aspects of the subject. No report of an experimental investigation was found. Despite the rigor of the theoretical solution, an experimental investigation showing agreement between the theory and test results would increase confidence in the correctness of the theory, even if the experimental verification was for but one condition of loading and restraint. There are other reasons for an experimental study of the subject. While the average of the results of a number of tests to determine the critical stress might agree well with the theoretically determined value, the difference in individual results are also of importance as indicating the variations that may be encountered. The problem of determining the critical load for a deep rectangular beam does not readily yield to a theoretical solution when buckling occurs at stresses beyond the elastic range of the material. Determination of critical loads in this plastic range of stresses, from test results, would permit an empirical extension of the results of theoretical analysis for elastic buckling that would be of value in deriving an expression for allowable working stresses in such beams. Such test results might also suggest a theory for the buckling of deep beams in the plastic range.

Deep rectangular beams may be either of solid section or hollow. A brief study of the stability of hollow rectangular beams was included in this investigation, with a few tests made to corroborate the theory.

The object of this investigation was to study the lateral instability of deep rectangular beams under various conditions of loading and restraint, with the view to determining an expression for allowable design stresses for such beams. The investigation included both analytical and experimental studies and dealt with solid and hollow rectangular beams.

## ANALYTICAL CONSIDERATION

### Solid Section

The theory of the elastic instability of deep rectangular beams is very well and completely presented by Timoshenko (reference 6, pp. 239-256) and by Prescott (reference 5, pp. 499-529). Both arrive at substantially the same expression for the critical bending moment at which the beam becomes unstable. This expression may be written

$$M_{cr} = \frac{K\sqrt{EI_zGJ}}{L} \qquad (1)$$

where $M_{cr}$ is maximum bending moment in the beam, in.-lb.

$E$, modulus of elasticity*, lb. per sq. in.

$I_z$, moment of inertia of the section about the greater axis, in.$^4$

---

*Timoshenko uses the value for Young's modulus of elasticity, while Prescott uses the "plate" modulus $E' = \frac{E}{1-\mu^2}$, where $\mu$ is Poisson's ratio. This difference will be discussed later in connection with the test results.

$G$, modulus of rigidity, lb. per sq. in.

$J$, section factor for torsional rigidity, in.$^4$

$L$, span length, in.

and $K$, constant depending on the conditions of loading and lateral support.

For the solid rectangular section, the section factor for torsion may be expressed

$$J = \beta b^3 d \tag{2}$$

where $b$ is width of rectangle, in.

$d$, depth of rectangle, in.

and $\beta$, constant depending on the ratio $d/b$.

Some values for $\beta$, as given by Timoshenko (reference 7), for ratios of $d/b$ representing "deep" rectangles are given in the following table:

| $\frac{d}{b}$ | 6 | 8 | 10 | $\infty$ |
|---|---|---|---|---|
| $\beta$ | 0.299 | 0.307 | 0.313 | 0.333 |

Perhaps a fair average value for $\beta$ in the study of deep rectangular beams would be 0.31.

Then

$$J = 0.31 b^3 d \tag{2a}$$

Further,

$$I_z = \frac{b^3 d}{12} \tag{3}$$

and, since $\mu = 1/3$ (for aluminum alloys)

$$G = \frac{3}{8} E$$

Now,

$$S = \frac{Mc}{I} \tag{4}$$

where $S$ is stress at outer fiber, lb. per sq. in.

$M$, bending moment, in.-lb.

$c$, distance from neutral axis to outer fiber, in., $c = d/2$

and $I$, moment of inertia of section about the short axis

$$I = \frac{bd^3}{12} \tag{5}$$

The expression for the critical stress in a deep rectangular beam may then be written

$$S_{cr} = K'E \frac{b^2}{Ld} \tag{6}$$

where $S_{cr}$ is maximum tension or compression in the beam

and $K'$, a constant depending on the conditions of loading and lateral support; $K' = 0.591\ K$

This expression is, of course, valid only when buckling occurs at stresses within the elastic range of the material.

Values for the constants $K$ and $K'$ are listed in table I for various conditions of loading and lateral support, for deep rectangular beams of one span. Some of these coefficients were obtained from sources previously mentioned, while others, which could not be found in the literature, were determined by the authors. A brief discussion of the methods employed and the calculations for one case may be found in the appendix.

The constants in table I apply when the load is considered as applied at the neutral axis of the beam. If, instead of being applied at the neutral axis, the load acts at the top of the beam, the critical stress is somewhat lower. For the case of a concentrated load applied to the top of a deep rectangular beam at the center of the span, Timoshenko (reference 6, p. 255) gives the following approximate expression for the value of the critical load:

$$P_{cr} = \frac{16.93 \sqrt{EI_z JG}}{L^2}\left(1 - \frac{1.74d}{L}\sqrt{\frac{EI_z}{JG}}\right) \qquad (7)$$

in which the terms are as previously defined. The first term of this expression is for the critical load when applied at the neutral axis of the beam. The second term in the parenthesis represents the reduction in the critical load when applied at the top of the beam. For very deep rectangular beams this term may be simplified by substitution $\left(\text{setting } J = \frac{b^3d}{3}\right)$ to read

$$1.42 \frac{d}{L} \qquad (7a)$$

Therefore, when the concentrated load is applied at the top of the beam, the constants given in table I for case 1 should be multiplied by the coefficient

$$\left(1 - 1.42 \frac{d}{L}\right) \qquad (7b)$$

A similar expression for the uniformly distributed load (case 7) applied to the top of the beam can also be obtained from Timoshenko's work. (See reference 3.) For this case the coefficient is

$$\left(1 - 1.26 \frac{d}{L}\right) \qquad (8)$$

## Hollow Section Rectangular Tube

The problem of the lateral stability of a hollow rectangular beam has not been treated in any of the available literature on the subject of lateral instability of beams probably because lateral buckling is uncommon in such beams. Fundamentally, the problem is the same as for a solid rectangular section, stability being provided by a combination of the torsional and lateral flexural stiffness of the beam. Expressions for the moments of inertia and the section factor for torsion are, of course, different in the case of the hollow rectangle. Also, in addition to the torsional stiffness of the beam (GJ), any tendency to twist is opposed by the bending resistance of the side walls of the tube in their own planes. For ordinary long beams, however, this latter consideration can safely be neglected. The expression for the section factor for torsion for a hollow rectangle may be written (reference 5, p. 166):

$$J = 2\,\frac{t t_1\ (b-t)^2 (d-t_1)^2}{bt + dt_1 - t^2 - t_1^2} \tag{9}$$

where $t$ is thickness of side walls, in.

$t_1$, thickness of top and bottom walls, in.

and $b$ and $t$ are as previously defined

This expression may be simplified, if the tubing is of uniform wall thickness, to read

$$J = 2\,\frac{t(b-t)^2 (d-t)^2}{b + d - 2t} \tag{9a}$$

and, if $t$ is negligibly small compared with $b$ and $d$, may be further simplified to

$$J = \frac{2b^2 d^2 t}{b + d} \tag{9b}$$

The moment of inertia about the long axis will be

$$I_z = \frac{b^3 d}{12} - \frac{(b-2t)^3 (d-2t)}{12} \tag{10}$$

and the moment of inertia about the short axis

$$I_y = \frac{bd^3}{12} - \frac{(b-2t)\ (d-2t)^3}{12} \tag{11}$$

Again, if $t$ is negligibly small compared with $b$ and $d$, these expressions may be written

$$I_z = \frac{b^2 t}{2}\left(d + \frac{b}{3}\right) \tag{10a}$$

and

$$I_y = \frac{d^2 t}{2}\left(b + \frac{d}{3}\right) \tag{11a}$$

For a hollow rectangular beam in which the wall thickness is negligibly small compared with the width and depth of the section, an expression for the critical stress can be written similar to equation (6) for the solid section. This expression is

$$S_{cr} = K''E\,\frac{b^2}{L}\left(\frac{3}{3b+d}\sqrt{\frac{3d+b}{3(b+d)}}\right) \tag{12}$$

where

$$K'' = K\sqrt{3/8} = 0.613K$$

A comparison between the stress at which lateral instability would occur in a solid and a hollow deep rectangular beam of the same outside dimensions may be obtained by considering first a beam with a ratio of width to depth of 1/6. Then the $\beta$ in equation (2) will be 0.299 and the $K'$ value in equation (6) will become

$$K' = 0.580\ K$$

and for the solid section

$$S_{cr} = 0.580\ KE\,\frac{b^2}{Ld}$$

For the hollow section

$$S_{cr} = 0.613\ KE\,\frac{b^2}{L}\left(\frac{3}{3b+d}\sqrt{\frac{3d+b}{3(b+d)}}\right)$$

The ratio of the critical stresses will then be

$$\frac{\dfrac{0.580}{d}}{0.613\left(\dfrac{3}{3b+d}\sqrt{\dfrac{3d+b}{3(b+d)}}\right)}$$

Then if $b = 1$ and $d = 6$, the critical stress for the hollow section will be 2.01 times the critical stress for the solid section provided, of course, that both beams buckle within the elastic range.

For a very deep beam ($b$ very small compared with $d$) the $\beta$ value will approach 1/3 and $K'$ will be the same as $K''$. If $b$ in the foregoing expression is neglected, the ratio of the critical stress in the hollow and the solid beams will be about 3 to 1.

When making these comparisons between the stability of beams of hollow and solid rectangular sections of the same outside dimensions, it must be remembered that the comparisons are on the basis of critical stress and not critical bending moment. If the beams are compared on the basis of critical bending moment (section modulus × critical stress), the solid beam, of course, will always carry the greater moment.

## MATERIAL AND DESCRIPTION OF TESTS

The material for this investigation consisted of 17ST aluminum alloy rolled rectangular bar with square corners and 17ST square-corner rectangular tubing. The nominal dimensions and the average tensile properties and compressive yield strengths of the bars and tubing are shown in table II.

The tensile properties of the material were determined from standard A.S.T.M. sheet specimens or round threaded-end test specimens depending on the thickness of the material. Both the tensile and compressive yield strength correspond to the stress that produced a permanent set of 0.2 percent. The tensile yield strengths were determined from load-strain curves drawn by an automatic autographic extensometer; the compressive yield strengths, from ordinary stress-strain curves.

The rectangular bars were tested in pairs as beams on edge as shown in figure 1. Each pair of bars was securely bolted to channel spreaders of approximately the same depth as the bars. These spreaders held the ends of the bars vertically and also prevented the bars from deflecting laterally. Figure 2 shows the arrangement of the ends of the specimens and the method of applying the loads. The span length for the $\frac{1}{2}$- by 2-inch bar and the $\frac{3}{4}$- by 2-inch bar varied from 36 to 96 inches and for the other bars, from 48 to 120 inches. In every case the unsupported length of the bars (length of bar subjected to uniform bending moment) was 24 inches less than the span length. In each of the tests the vertical deflection of both the bars was measured at the center of the span by means of a mirrored scale and taut wires. Lateral deflections of the bars were measured from a reference mark on the top edge of each bar at midspan to fixed points in the testing machine with a scale graduated to 0.01 inch. While this method of measuring lateral deflection was satisfactory for these tests, it obviously made no distinction between lateral movement and rotation of the bars. Both the vertical and lateral deflections of the bars were measured for various increments of load until failure occurred by lateral buckling or until the extreme fiber stress, as computed by the flexure formula, was appreciably greater than the yield strength of the material. In the case of the $\frac{1}{2}$- by 6-inch bars over a span length of 48 inches, the capacity of the machine was reached before lateral buckling occurred although the data indicated that such failure was impending.

Huggenberger extensometers were used to measure the maximum fiber stresses at the lower loads. These instruments were attached to the top and bottom edges of both bars about 6 inches from the middle of the span. No attempt was made to measure stresses up to failure because of the possibility of damage to the instruments in case of sudden failure.

## DISCUSSION

### Test Results

The results of the beam tests are summarized in table III. This table shows the computed stress at failure and the type of failure for each test. Failure occurred in three distinct ways: vertical yielding, vertical yielding accompanied by lateral buckling, and lateral buckling alone. Typical load-deflection curves for these three types of failures are shown in figures 3, 4, and 5. Figure 3 shows the vertical and lateral deflection data for a $\frac{1}{2}$- by 2-inch beam stressed beyond the yield strength of the material. The departure of the vertical deflection curve from a straight line was considerable, whereas the lateral deflection was zero throughout the test. While bars in this class have been described as failing by vertical yielding, it should be pointed out that, had loading been continued, ultimate failure would probably have occurred by lateral buckling in many cases. The test was stopped when the stress in the outer fiber had appreciably exceeded the yield strength of the material. The nature of the failure when the apparent outer fiber stress in the beam $\left(S = \frac{Mc}{I}\right)$ has exceeded 45,000 pounds is not of extreme importance since for such beams the nominal design stress of 15,000 pounds per square inch (17ST) represents a factor of safety of at least 3. Figure 4 shows the deflection data for a 3/8- by 4-inch beam. In this case the beam was yielding in the vertical direction as evidenced by the departure of the load-deflection curve from a straight line, and failure occurred by lateral buckling. That lateral buckling occurs at a very definite stress is evident from the sharp break in the lateral deflection curves. Figure 5 shows representative deflection curves for the specimens that failed by lateral buckling without yielding in the vertical plane.

The critical stress at which the rectangular bars failed by lateral buckling, both in the elastic range and beyond, have been plotted in figure 6 in comparison with the curve representing the calculated values for critical stress.

It is not surprising that the rectangular tube showed no indication of lateral buckling. Based on the analysis of a preceding section and employing equations (9a), (10), and (11), the calculated value for critical stress, assuming elastic action, is about 186,000 pounds per square inch. The critical stress for a solid bar of the same outside dimensions and loaded in the same manner would be 124,000 pounds per square inch. Neither of these values is significant as indicating the strength of the beams since failure would occur by yielding instead of by lateral buckling. A comparison of these critical stress values, however, indicates that, for beams of these proportions (ratio of b/d of 1/4), the critical stress for the hollow tube is about 50 percent greater than for the solid bar, provided they buckle elastically. For elastic buckling to occur in a rectangular beam of such proportions, the beam would have to be extremely long, and considerable deflections in the plane of the loads would be produced before lateral buckling occurred. If this deflection is considered, the coefficient K is found to be not a constant but dependent on the ratio of b/d, being larger for the wider beams. (See reference 6, p. 248.)

When tested over a span length of 120 inches, the rectangular tubes yielded in the vertical plane with no indication of lateral buckling as is shown in figure 7. Loading of the tubes was discontinued when the vertical deflection at the middle of the span was 3-1/4 inches.

## Failure by Elastic Buckling

The lower straight-line portion of the curve in figure 6 represents the equation

$$S = 3.71 \times 10.3 \times \frac{b^2}{Ld} \times 10^6 \qquad (13)$$

which is equation (6) with the K' value for case 2 (table I). The conditions of this case were faithfully reproduced in the tests. The agreement between this curve and the points representing failure by elastic buckling is quite satisfactory, particularly when it is remembered that the tests were made on beams of different sizes.

Also in figure 6 is shown the straight line representing the equation

$$S = 3.71 \times 10.9 \frac{b^2}{Ld} \times 10^6 \qquad (14)$$

In the derivation of this equation, the value E in equation (1) was replaced by the plate modulus E',

$\left(E' = \dfrac{E}{1-\mu^2}\right)$, while the value for G remained unchanged. (See reference 5, pp. 499-529.) The difference in slope of these two lines is only about 6 percent. The points representing experimentally determined values of critical stress fall below the upper line, indicating that perhaps the plate modulus value is not applicable to beams of the proportions of those tested. It is probable that for beams of extremely deep and narrow section the critical stress would be slightly greater than the calculated value based on a modulus value of 10,300,000 pounds per square inch.

A study of the values of the constant K' given in table I for various conditions of loading and restraint indicates the importance of considering the type of loading as well as the nature of the restraint in calculating the critical stress for a deep rectangular beam. For instance, a comparison of the value of K' for cases 1, 5, and 8, shows that for a simple span with the ends of the beam held vertical the critical stress for a uniformly distributed load is 12 percent greater and for a concentrated load at the center of the span is 35 percent greater than when the beam is subjected to pure bending. If, however, the ends of the beam are clamped in the horizontal plane (cases 2, 6, and 9), there is very little difference in the critical stress under the different loading conditions, being lowest for the distributed load. But, if the lateral restraint consists of holding the beam vertical at the ends and at the middle of the span (cases 3, 7, and 10), the critical stress for the distributed load is 31 percent greater and for the concentrated load, 77 percent greater than for pure bending. Another instance of the importance of considering the nature of the load is afforded in a comparison of the K' values for cases 14 and 16 or cases 13 and 15. Such a comparison reveals that the critical stress for a deep rectangular beam loaded as a cantilever with a uniformly distributed load acting along its neutral axis is about 60 percent greater than for a similar beam loaded with a concentrated load at the free end, provided, of course, that buckling occurs within the elastic range.

An interesting point is brought out by a comparison of the K' values for cases 9 and 13, which indicates that a deep rectangular beam built in at the ends and subjected to a concentrated load at the middle of the span will fail by lateral buckling at a stress lower than the critical stress for a similar beam, loaded in the same manner, simply supported in a vertical plane but restrained at the ends against lateral deflection. The critical load for the built-in beam will be greater than for the simply supported beam (case 8), but will be less than twice as great.

The effect of the position of the applied load, relative to the neutral axis on the lateral stability of a deep rectangular beam, has been discussed. It is evident from equations (7) and (8) that this consideration becomes of great importance for short spans.

## Stress Distribution and Buckling Beyond the Elastic Range

When the stress in the outer fiber of the beam exceeds the proportional limit of the material, the expression $S = \frac{Mc}{I}$ no longer represents the true condition of stress. For a beam of rectangular cross section, however, it is not difficult to derive an expression for the stress at the outer fiber if it is assumed that (1) the material of the beam is homogeneous and has the same stress-strain relationship in tension and compression, (2) that plane sections remain plane (i.e., the strain is proportional to the distance from the the neurtral axis), and (3) all longitudinal fibers of the beam are in simple tension or compression.

The stress-strain curve shown in figure 8 may also be considered as a curve of the stress distribution on the upper or lower half of the cross section of a rectangular beam if the axis representing stress is taken as the neutral axis of the beam and the strain axis as the vertical center line of the cross section. The depth of the beam is arbitrary, and half of the depth may be represented by any distance on the strain axis depending on the stress conditions for the particular case. If half the depth of the beam is considered to be represented by a certain distance from the neutral axis, as indicated in figure 8, and it is assumed that a beam of unit width is being dealt with, the moment about the neutral axis of the area bounded by the stress-strain curve and the line representing the outer fiber of the beam, when properly corrected for the stress and depth scales, represents one-half the resisting moment offered by a beam of rectangular cross section of unit width and of twice unit depth for that particular value of stress at the outer fiber. This resisting moment, which shall be called $R$, has been determined from the curve in figure 8 for different values of stress $S$ at the outer fiber. These results have been listed in table IV and plotted in figure 9. In figure 9 it is evident that the relation between $S$ and $R$ may be very closely represented by two straight lines as shown. The lower portion represents the relationship

$$S = 3R \tag{15}$$

and applies for values of $S$ less than 26,000 pounds per square inch. For stresses greater than 26,000 pounds per square inch the relationship is expressed by the equation

$$S = 12{,}500 + 1.56R \tag{16}$$

Since $R$ represents one-half the resisting moment of a beam of rectangular section of unit width and twice unit depth, the total resisting moment of a rectangular section of width $b$ and depth $d$ can be shown by scalar expansion to be

$$M = \frac{R}{2}\,bd^2 \quad \text{or} \quad R = \frac{2M}{bd^2} \tag{17}$$

Then the maximum fiber stress within the elastic range will be

$$S = 3R = \frac{6M}{bd^2} \tag{18}$$

which coincides with the expression given by the equation

$$S = \frac{Mc}{I} \tag{19}$$

When stresses greater than 26,000 pounds per square inch are involved, the actual value for the maximum fiber stress may be obtained from the expression

$$S = 12{,}500 + \frac{3.12\ M}{bd^2}$$

If the value of the stress as determined by the flexure formula $\left(S = \frac{Mc}{I}\right)$ is called the "apparent stress" and represented by $S_A$, then for values greater than 26,000 pounds per square inch, actual stress may be expressed in terms of the apparent stress as follows:

$$S = 12,500 + 0.52\, S_A \tag{20}$$

or

$$S_A = \frac{S - 12500}{0.52} \tag{20a}$$

A consideration of the stress distribution across the section affords a logical means for determining the critical load on a deep rectangular beam when stressed beyond the elastic range. If it is assumed that the ratio between the modulus of elasticity $E$ and the modulus of rigidity $G$ remains unchanged, the apparent critical stress $S_A$ may be obtained from equation (6) provided the proper value for the effective modulus $E$ is used. The value for the effective modulus used in determining the portion of the curve in figure 6, representing lateral buckling beyond the elastic range, was obtained as the average modulus for all the elements of a cross section corresponding to a particular value of stress on the outer fiber. For the case of pure bending, the stress distribution on all cross sections of the beam are the same. By definition, the modulus of elasticity is the ratio of change in stress to change in strain. Consequently, the modulus at any given stress is the slope of the stress-strain curve at that stress. This modulus value, aptly called the "tangent" modulus, has been plotted in figure 10 for the stress-strain curve shown in figure 8. The average modulus for the beam for a particular value of stress at the outer fiber would then be the average ordinate of the portion of the tangent-modulus curve below that stress. This average modulus curve has also been plotted in figure 10. Since it is convenient to deal in terms of apparent rather than actual stress at the outer fiber, the average modulus curve has also been plotted against apparent stress in figure 10. Values from this curve have been used in determining the critical stress curve of figure 6. The relation between apparent outer fiber stress and average modulus can be represented by a straight line. The equation for this straight line is

$$E_A = 12,550,000 - 102\, S_A \tag{21}$$

and from equation (6), the critical apparent stress may be expressed

$$S_A = \frac{12550000 \left(K' \frac{b^2}{Ld}\right)}{1 + 102 \left(K' \frac{b^2}{Ld}\right)} \tag{22}$$

This equation is applicable for stresses greater than 22,000 pounds per square inch and permits a direct determination of the critical apparent stress.

It is recognized that this value for the effective modulus cannot be rigidly justified by theoretical considerations. It can be shown, however, that the critical stress calculated on the basis of a more rigid theoretical consideration of the lateral flexural and torsional rigidity of the beam, which would include an involved expression for the effective modulus, will be slightly greater than the value obtained using this simplified effective modulus value. It is significant to note the agreement between the calculated critical stress curve thus obtained and the experimental results (figure 6).

It might be pointed out that this value for effective modulus applies only in the case of pure bending. For other types of loading, such as concentrated or distributed loads, where the distribution of stress on a cross section varies throughout the length of the beam, it would be necessary to consider the variation in average modulus for different sections. In such cases, the effective modulus corresponding to a particular value of apparent stress (beyond the elastic range) would be greater than for pure bending.

As may be seen in figure 6, the curve representing the critical apparent stress beyond the elastic range may be closely approximated by a straight line. The critical stress for the case of a deep rectangular beam of 17ST aluminum alloy subjected to pure bending with the ends fixed against lateral deflection may be determined from the equations for the two straight lines. For $\frac{b^2}{Ld} \times 10^{-6}$ values from 0 to 680,

$$S = 38.2 \times 10^6 \times \frac{b^2}{Ld} \tag{23}$$

For values of $\frac{b^2}{Ld} \times 10^{-6}$ ranging from 680 to 1,500

$$S_A = 10{,}000 + \left(23.2 \times 10^6 \frac{b^2}{Ld}\right) \qquad (24)$$

where $S_A$ is the apparent stress on the outer fiber

$$\left(S_A = \frac{Mc}{I}\right)$$

## CONCLUSIONS

From this study of the lateral stability of deep rectangular beams, the following conclusions may be drawn:

1. The stress at which a deep rectangular beam becomes unstable within the elastic range of the material may be determined from the equation

$$S = K'E \frac{b^2}{Ld} \qquad (6)$$

2. In the determination of the critical stress for a deep rectangular beam, it is important to consider the nature of the load as well as the manner in which the beam is supported.

3. For a long deep rectangular tube in which the wall thickness is uniform and is small compared with the width and depth, the critical stress within the elastic range may be expressed

$$S = K'E \frac{b^2}{L} \left(\frac{3}{3b+d} \sqrt{\frac{3d+b}{3(d+b)}}\right) \qquad (12)$$

4. Depending on the ratio of b/d, the critical stress for a thin-walled deep rectangular tube may be as much as three times as great as the critical stress for a solid rectangular beam of the same dimensions, loaded and supported in the same manner. For a ratio of b/d of 1/4, the critical stress for the tube would be about 50 percent

greater than for a solid bar of the same size provided buckling occurred elastically.

5. The critical stress, as determined experimentally for solid deep rectangular beams subjected to pure bending with their ends restrained against lateral deflection, agreed very well with the values determined analytically.

6. For deep rectangular beams of solid section subjected to pure bending beyond the elastic range of the material, the critical apparent stress may be calculated from $S = K'E \frac{b^2}{Ld}$, using as the value of E the average tangent modulus for all the elements of the cross section. For a rectangular bar of 17ST, this average modulus value may be expressed by

$$E_A = 12550000 - 102\ S_A \tag{21}$$

where

$$S_A = \frac{Mc}{I} > 22,000$$

and the critical apparent stress may be expressed by

$$S_A = \frac{12550000\ \left(K' \cdot \frac{b^2}{Ld}\right)}{1 + 102\ \left(K'\ \frac{b^2}{Ld}\right)} \tag{22}$$

7. The critical apparent stress for values between the limit of the elastic range and a value of 45,000 pounds per square inch, as determined by tests on deep rectangular bars subjected to pure bending with their ends restrained against lateral deflection, was in agreement with values calculated by equations (6) and (22).

## APPENDIX

Since lateral buckling of a deep rectangular beam consists of a combined lateral deflection and twisting of the beam, both the flexural and torsional stiffness of the beam must be considered in determining its limit of stability. If axes are taken as shown in figure 11 and the angle of rotation is expressed as $\theta$, the differential equations of equilibrium for the lateral bending and the twisting of the beam may be written

$$EI_z \frac{d^2y}{dx^2} = M_B \tag{25}$$

$$GJ \frac{d\theta}{dx} = M_T \tag{26}$$

where $EI_z$ is lateral flexural rigidity

$GJ$, torsional rigidity

$M_B$, lateral bending moment that can be expressed in terms of the external load and the angle $\theta$

$M_T$, twisting moment that can be expressed in terms of the external load and some function of the lateral deflection $y$

These equations may be reduced to a differential equation of the second order, first degree in $\theta$. When this differential equation has constant coefficients, as is the case when the beam is subjected to pure bending, it yields readily to an exact solution. If the equation has variable coefficients, a solution may be effected by the method of infinite series. This method of solution is frequently very laborious and, in many cases, where the curve $\theta = f(x)$ is of simple form, the equation may be more easily solved approximately by the method of finite differences. This method divides the length of the beam into equal intervals and assumes that three successive points are connected by a curve of parabolic form. The accuracy of this method is improved by increasing the number of intervals, but in many cases a solution of sufficient accuracy can be obtained with surprisingly little work. Obviously, such a method will not give very accurate results through a point of contraflexure. It has been found that values for critical stress determined by this method are somewhat lower than values given by the exact solution of the differential equation.

Another method that may be frequently used to advantage in the determination of the limit of lateral stability of a beam is the energy method used extensively by Timoshenko. In this method, the strain energy of lateral bending plus the strain energy of twist are equated to the work produced by the lowering of the external load caused by the lateral buckling. The expressions for the external work and the strain energy will involve functions of both $\theta$ and $y$. From the equilibrium equations (25) and (26), however, one or the other of these variables can be eliminated. Solution of the equation is then accomplished by assuming a function of the variable that satisfies the boundary conditions and effecting the integrations involved. If the function of the variable assumed is the correct one, the critical load thus determined will agree exactly with the value determined from an exact solution of the differential equation. For any other function, however, the critical load determined by the energy method will invariably be higher than the exact solution. The strain-energy method was found to be particularly useful in cases involving distributed load and when the beam was restrained against lateral deflections. An analysis of the effect on the stability of the beam of a displacement of the load above or below the neutral axis can also be readily made using this method.

As an example of the use of the strain-energy method, calculations will be given for the critical value of a uniformly distributed load applied at the neutral axis of a simply supported deep rectangular beam, the ends of which are held vertical and restrained against lateral deflection. Consider the beam shown in figure 12, loaded with a uniformly distributed load of $w$ (lb. per sq. in.) acting at the neutral axis with the coordinate axes disposed as indicated. The lateral end restraining moment $N$ is such that the slope of the lateral deflection curve at the ends is zero; i.e.,

$$\frac{dy}{dx} = 0$$

where $x = \pm L$.

The expression for the strain energy of bending can be written (reference 7, pp. 303-306)

$$V_B = EI_z \int_0^L \left(\frac{d^2y}{dx^2}\right)^2 dx \tag{27}$$

and the strain energy in torsion can be expressed

$$V_T = GJ \int_0^L \left(\frac{d\theta}{dx}\right)^2 dx \tag{28}$$

The work done by the external load corresponding to the strain energy of bending and twisting can be expressed (reference 3)

$$W = w \int_0^L \theta \left(\frac{d^2y}{dx^2}\right) (L^2 - x^2)\, dx \tag{29}$$

Then the equation representing the balance between external and internal energy becomes

$$w \int_0^L \theta \left(\frac{d^2y}{dx^2}\right)(L^2 - x^2)\, dx = GJ \int_0^L \left(\frac{d\theta}{dx}\right)^2 dx + EI_z \int_0^L \left(\frac{d^2y}{dx^2}\right)^2 dx \tag{30}$$

For these conditions of loading and restraint equation (25) becomes

$$EI_z \frac{d^2y}{dx^2} = \frac{w}{2} (L^2 - x^2)\, \theta - N \tag{31}$$

At this point the assumed expression from the function of $\theta$ is introduced. An equation of the form

$$\theta = A\left(1 + \cos \frac{\pi x}{L}\right) \tag{32}$$

satisfies the boundary conditions, which are

$$x = \pm L \qquad \theta = 0 \qquad \frac{d\theta}{dx} = 0$$

$$x = 0 \qquad \theta = 0 \qquad \frac{d\theta}{dx} = 0$$

Then equation (31) becomes

$$EI_z \frac{d^2y}{dx^2} = \frac{w}{2} A\left(1 + \cos\frac{\pi x}{L}\right)(L^2 - x^2) - N \tag{33}$$

Since $dy/dx = 0$ at $x = 0$ and $x = L$,

$$\int_0^L \frac{d^2y}{dx^2}\,dx = 0 \tag{34}$$

If for $\frac{d^2y}{dx^2}$ its value from equation (33) be substituted, the restraining moment N can be evaluated. It is found that

$$N = 0.4347\ wAL^2 \tag{35}$$

The terms $\frac{d^2y}{dx^2}$ and $\left(\frac{d^2y}{dx^2}\right)^2$ in equation (30) can now be replaced by expressions involving $\theta$ as the only variable. Terms involving any function of $\theta$ can in turn be replaced by their equivalent from equation (32). Equation (30) is thus reduced to the form

$$\frac{w^2}{4EI_z}\int_0^L \left[(L^2 - x^2)^2\left(1 + \cos\frac{\pi x}{L}\right)^2 - 0.7558L^4\right] dx =$$

$$\frac{GJ\pi^2}{L^2}\int_0^L \sin^2\left(\frac{\pi x}{L}\right) dx \tag{36}$$

Performing the indicated integrations and simplifying,

$$wL_{CR} = 6.11\sqrt{\frac{EI_zGJ}{L^2}}$$

Aluminum Company of America,
Aluminum Research Laboratories,
New Kensington, Penna., Nov. 11, 1936.

## REFERENCES

1. Prandtl, L.: Kipperscheinungen. Dissertation, Nuremburg, 1899.

2. Michell, A. G. M.: Phil. Mag., vol. 48, 1899.

3. Timoshenko, S.: Annales des ponts et chaussees, 1913.

4. Timoshenko, S.: Strength of Materials, Part II. D. Van Nostrand Company, Inc., 1930.

5. Prescott, John: Applied Elasticity, Longmans, Green, and Company. (London), 1924.

6. Timoshenko, S.: Theory of Elastic Stability. McGraw-Hill Book Company, Inc. 1936.

7. Timoshenko, S.: Strength of Materials, Part I. D. Van Nostrand Company, Inc., 1930.

TABLE I

CONSTANTS FOR DETERMINING THE LATERAL STABILITY OF SOLID DEEP RECTANGULAR BEAMS

| CASE | SIDE VIEW | TOP VIEW | K | K' |
|---|---|---|---|---|
| 1 | 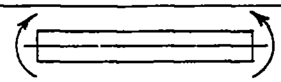 |  | 3.14 | 1.86 |
| 2 | 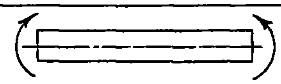 |  | 6.28 | 3.71 |
| 3 | 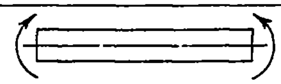 | 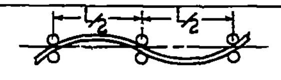 | 6.28 | 3.71 |
| 4 | 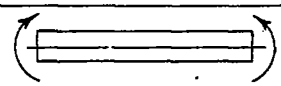 | 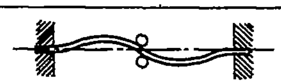 | 9.22 | 5.45 |
| 5 | 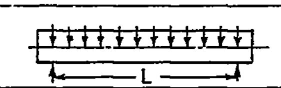 | 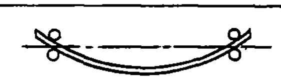 | 3.54 | 2.09 |
| 6 | 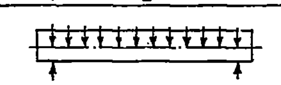 | 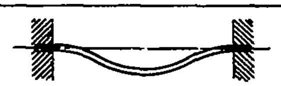 | 6.10 | 3.61 |
| 7 | 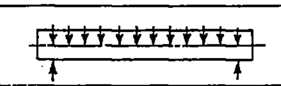 | 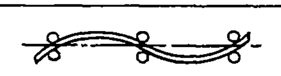 | 8.24 | 4.87 |
| 8 |  | 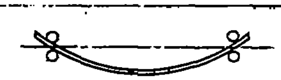 | 4.235 | 2.50 |
| 9 |  |  | 6.47 | 3.82 |
| 10 |  | 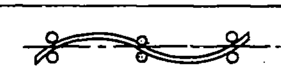 | 11.12 | 6.57 |
| 11 | 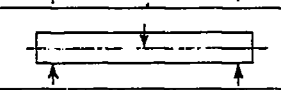 | 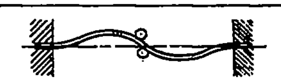 | 13.1 | 7.74 |
| 12 |  | 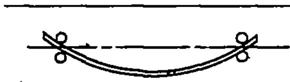 | 5.29 | 3.13 |
| 13 | 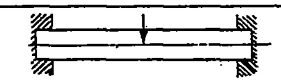 |  | 5.88 | 3.48 |
| 14 | 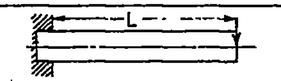 | 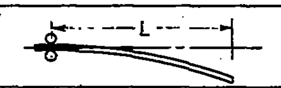 | 4.01 | 2.37 |
| 15 | 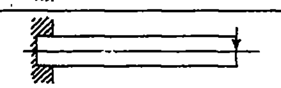 | 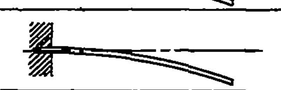 | 4.01 | 2.37 |
| 16 | 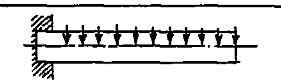 | 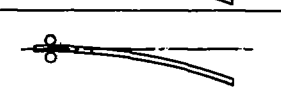 | 6.43 | 3.80 |
| 17 | 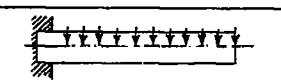 | 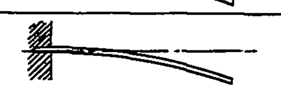 | 6.43 | 3.80 |

TABLE II

Nominal Dimensions and Mechanical Properties of Rolled Rectangular Bar and Rectangular Tubing

17ST Aluminum Alloy

| Section | Width (in.) | Depth (in.) | Yield strength (lb./sq.in.) | | Tensile strength (lb./sq.in.) | Elongation in 2 in. (percent) |
|---|---|---|---|---|---|---|
| | | | Tension | Compression | | |
| Bar | 1/2 | 2 | 40,400 | 33,800 | 55,530 | 24.3 |
| Bar | 3/4 | 2 | 40,900 | 33,000 | 55,400 | 25.1 |
| Bar | 1/4 | 4 | 40,160 | 35,000 | 56,520 | 24.2 |
| Bar | 1/2 | 4 | 37,800 | 34,000 | 56,400 | 24.2 |
| Bar | 3/8 | 4 | 37,550 | 33,900 | 54,340 | 25.5 |
| Bar | 1/2 | 6 | 36,500 | 33,700 | 55,930 | 26.6 |
| Tubing* | 1-1/4 | 5 | 38,600 | | 59,450 | 21.4 |

*Outside dimensions; wall thickness = 0.095 in.

TABLE III

SUMMARY OF TEST RESULTS

| Test | Actual size (in.) (d) Depth | Actual size (in.) (b) Width | Section modulus (in.$^3$) | Span Length (in.) | Unsupported length (L) (in.) | $\frac{b^2}{Ld}$ | Stress/1000 lb. load (lb./sq.in.) Measured | Stress/1000 lb. load (lb./sq.in.) Computed | Maximum applied moment (in.-lb.) | Maximum fiber stress (lb./sq.in.) Apparent | Maximum fiber stress (lb./sq.in.) Actual | Nature of failure |
|---|---|---|---|---|---|---|---|---|---|---|---|---|
| 1 | 2.007 | 0.750 | 1.018 | 96 | 72 | $3,893 \times 10^{-6}$ | 6,175 | 5,895 | 18,000 | 35,360 | 31,200 | Yielding |
| 2 | 2.012 | .750 | 1.011 | 72 | 48 | 5,624 | 6,170 | 5,935 | 21,000 | 41,540 | 34,200 | " |
| 3 | 2.012 | .748 | 1.009 | 48 | 24 | 11,586 | 6,160 | 5,945 | 24,000 | 47,570 | 37,300 | " |
| 4 | 2.002 | .748 | .999 | 36 | 12 | 23,289 | 6,175 | 6,005 | 24,000 | 48,050 | 37,300 | " |
| 5 | 1.994 | .496 | .657 | 96 | 72 | 1,713 | 9,525 | 9,130 | 10,800 | 32,880 | 29,300 | " |
| 6 | 1.994 | .496 | .658 | 72 | 48 | 2,570 | 9,250 | 9,120 | 13,500 | 41,030 | 32,800 | " |
| 7 | 1.994 | .497 | .659 | 48 | 24 | 5,061 | 9,300 | 9,105 | 13,500 | 40,970 | 32,800 | " |
| 8 | 1.998 | .498 | .662 | 36 | 12 | 10,344 | 8,850 | 9,065 | 18,000 | 54,380 | 40,300 | " |
| 9 | 3.993 | .501 | 2.662 | 120 | 96 | 655 | 2,350 | 2,255 | 33,000 | 24,780 | 24,780 | Lateral buckling |
| 10 | 4.000 | .502 | 2.675 | 96 | 72 | 875 | 2,350 | 2,240 | 41,700 | 31,180 | 28,700 | " " |
| 11 | 4.014 | .502 | 2.693 | 72 | 48 | 1,308 | 2,270 | 2,230 | 58,050 | 43,110 | 35,000 | Lateral buckling and yielding |
| 12 | 4.012 | .501 | 2.688 | 48 | 24 | 2,606 | 2,260 | 2,230 | 60,000 | 44,640 | 35,800 | Yielding |
| 13 | 6.023 | .500 | 6.053 | 120 | 96 | 432 | 1,020 | 990 | 51,600 | 17,050 | 17,050 | Lateral buckling |
| 14 | 6.010 | .500 | 6.025 | 96 | 72 | 578 | 1,040 | 995 | 67,050 | 22,260 | 22,620 | " " |
| 15 | 6.008 | .500 | 6.009 | 72 | 48 | 867 | 1,010 | 1,000 | 90,000 | 29,960 | 28,100 | " " |
| 16 | 6.006 | .499 | 6.001 | 48 | 24 | 1,727 | 1,015 | 1,000 | 120,000 | 39,990 | 33,200 | Lateral buckling and yielding |
| 17 | 3.997 | .376 | 2.003 | 120 | 96 | 369 | 3,090 | 2,995 | 13,200 | 13,170 | 13,170 | Lateral buckling |
| 18 | 4.002 | .377 | 2.012 | 96 | 72 | 490 | 3,125 | 2,980 | 19,230 | 19,120 | 19,120 | " " |
| 19 | 3.995 | .376 | 2.003 | 72 | 48 | 737 | 3,055 | 2,995 | 26,850 | 26,810 | 26,500 | " " |
| 20 | 3.999 | .375 | 1.999 | 48 | 24 | 1,465 | 3,055 | 3,000 | 44,400 | 44,420 | 35,500 | Lateral buckling and yielding |
| 21 | 3.986 | .253 | 1.343 | 120 | 96 | 167 | 4,660 | 4,470 | 4,425 | 6,580 | 6,580 | Lateral buckling |
| 22 | 4.016 | .254 | 1.362 | 96 | 72 | 223 | 4,585 | 4,405 | 5,580 | 8,190 | 8,190 | " " |
| 23 | 4.000 | .254 | 1.355 | 72 | 48 | 336 | 4,525 | 4,430 | 8,935 | 13,170 | 13,170 | " " |
| 24 | 3.994 | .254 | 1.350 | 48 | 24 | 673 | 4,525 | 4,445 | 17,400 | 25,780 | 25,780 | " " |
| 25 | 4.991 | 1.250 | 2.546 | 120 | 96 | — | 2,330 | 2,355 | 55,500 | 43,700 | — | Yielding |
| 26 | 4.992 | 1.251 | 2.543 | 96 | 72 | — | 2,395 | 2,355 | 54,000 | 42,430 | — | " |

TABLE IV

Values of Resisting Moment R
for Various Values of Stress at the Outer Fiber S
of a Bar of 17ST Aluminum Alloy

| Stress (lb./sq.in.) | Resisting Moment (in.-lb.) |
|---|---|
| 10.500 | 3,600 |
| 20,900 | 6,920 |
| 28,300 | 10,140 |
| 31,500 | 12,240 |
| 33,700 | 13,720 |
| 35,300 | 14,670 |
| 36,800 | 15,600 |
| 38,000 | 16,280 |

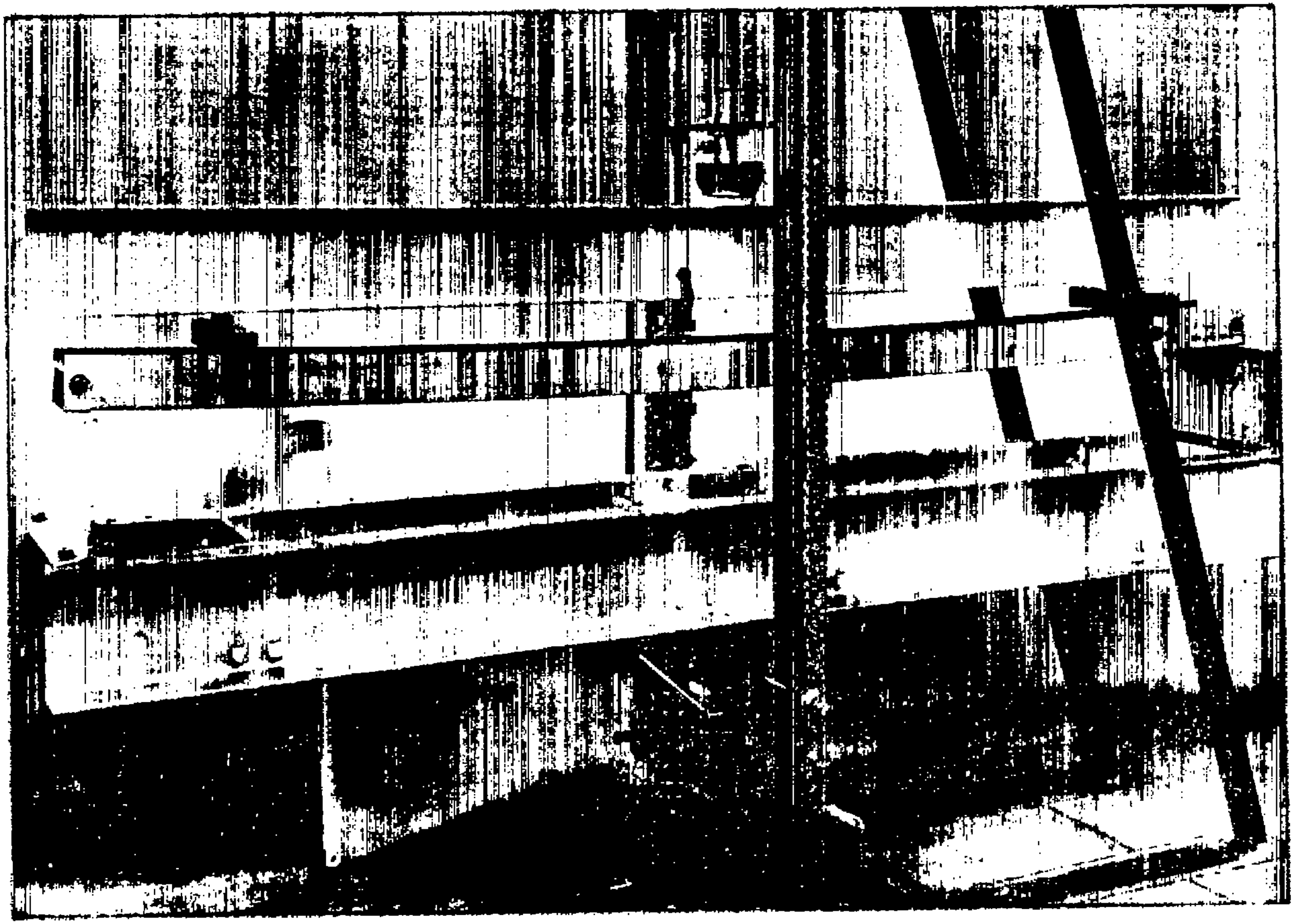

Figure 1.-Set-up for lateral instability test of deep rectangular bars.

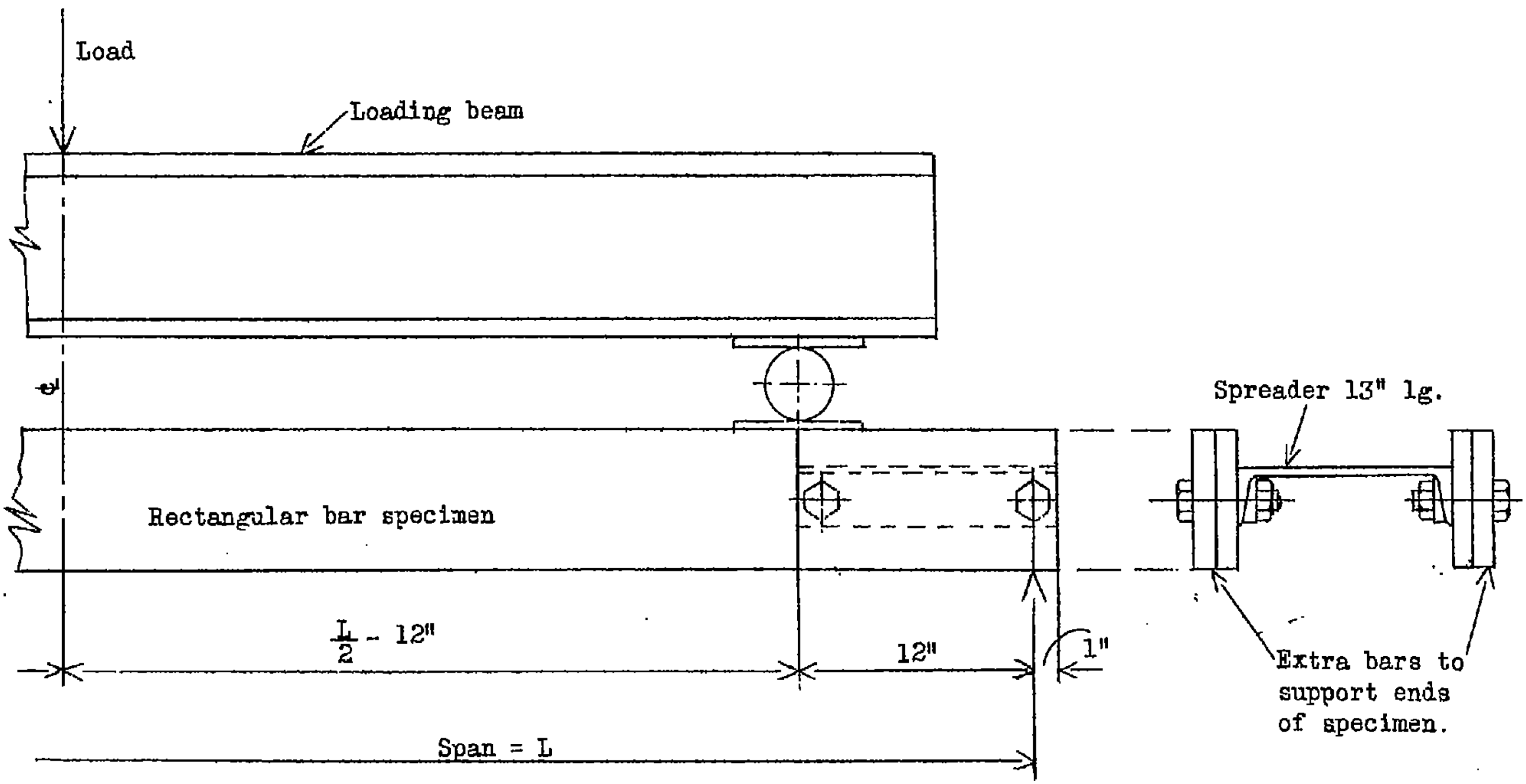


Figure 2.- Sketch of specimen for rectangular bar test.

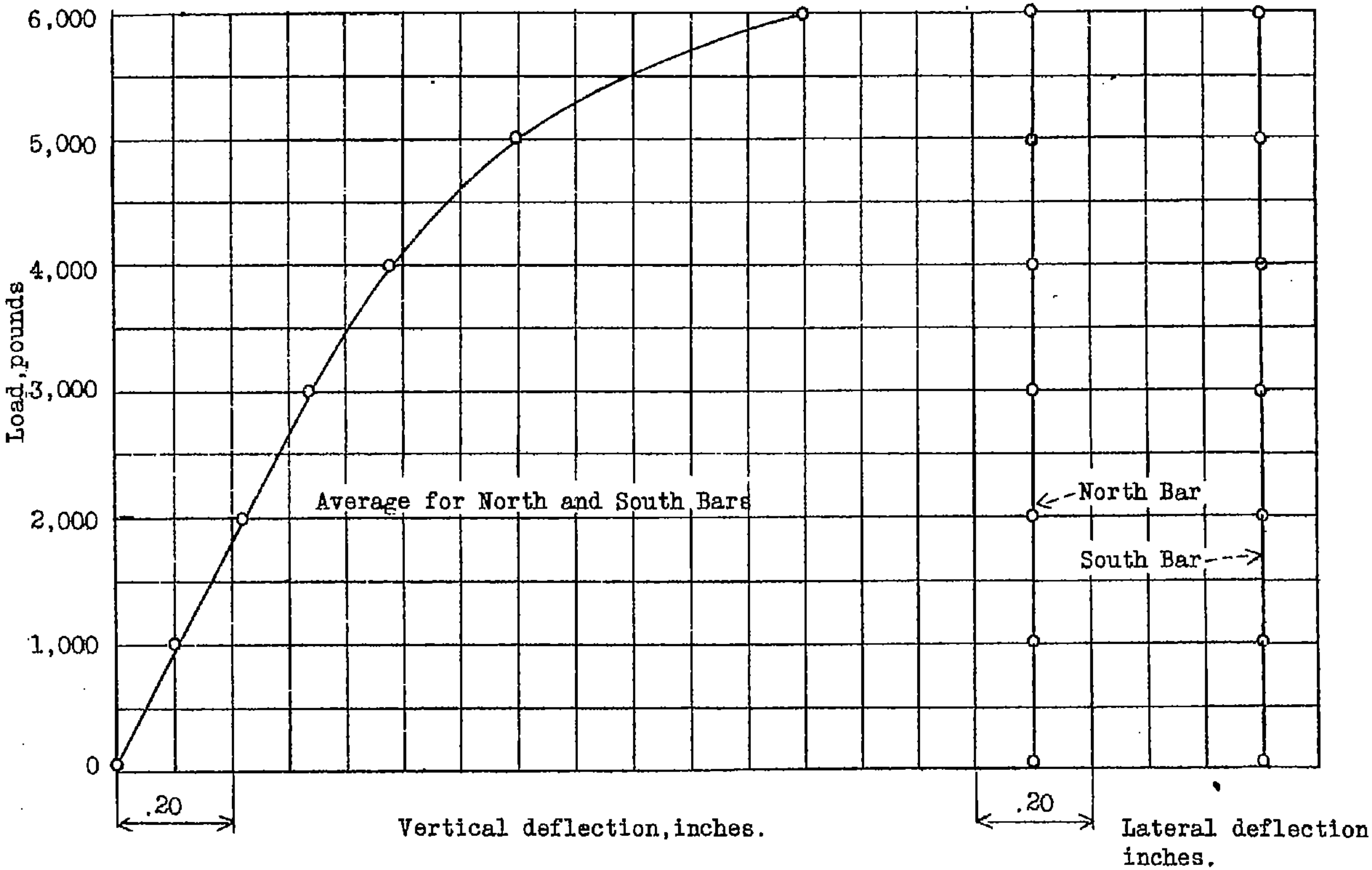


Figure 3.- Load-deflection curves for rectangular bars on edge. Span length, 36 in.; unsupported length, 12 in.; width, 1/2 in.; depth, 2 in.; 17ST aluminum alloy.

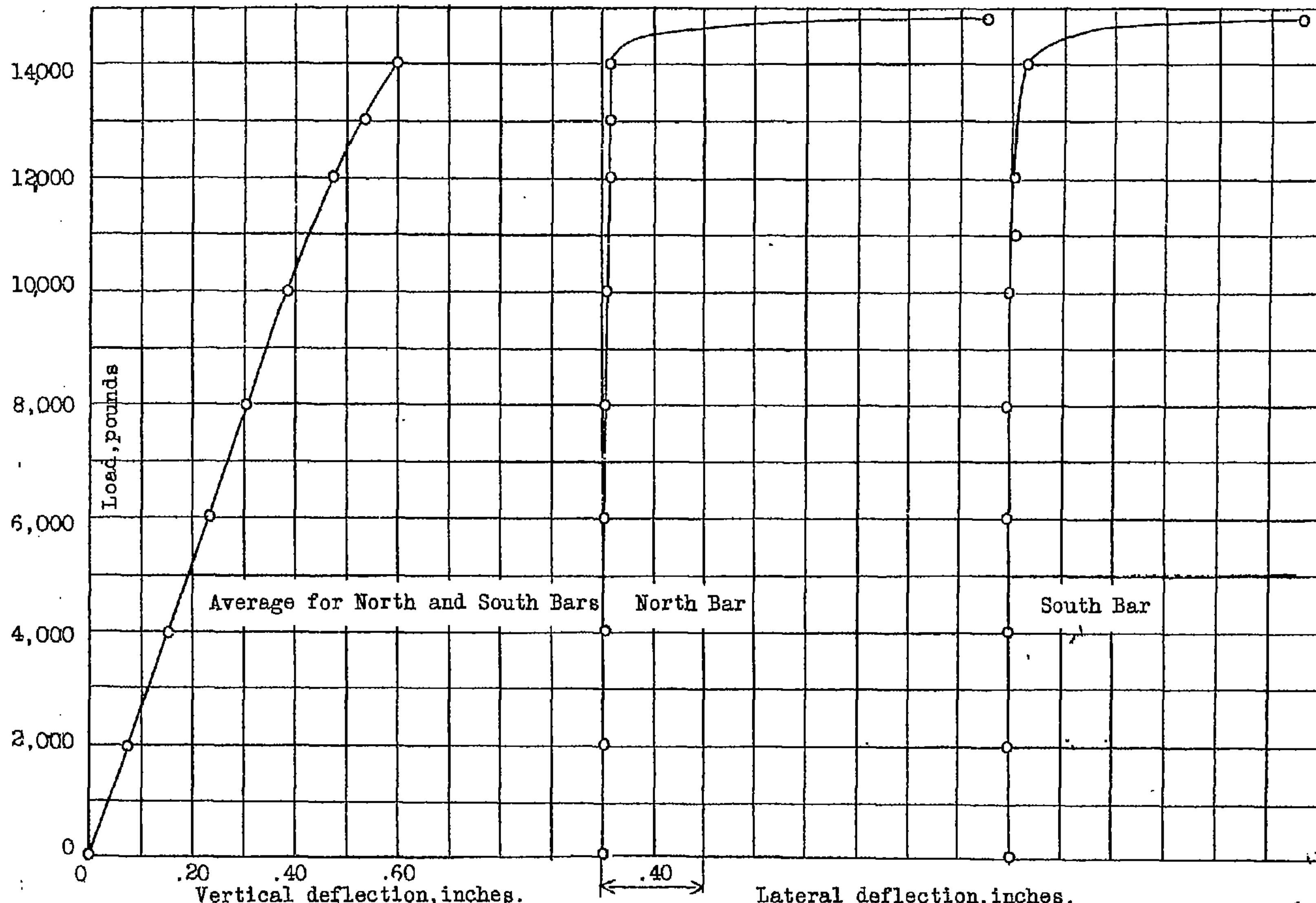


Figure 4.- Load-deflection curves for rectangular bars on edge. Span length, 48 in. unsupported length, 24 in.; width, 3/8 in.; depth, 4 in.; 17ST aluminum alloy.

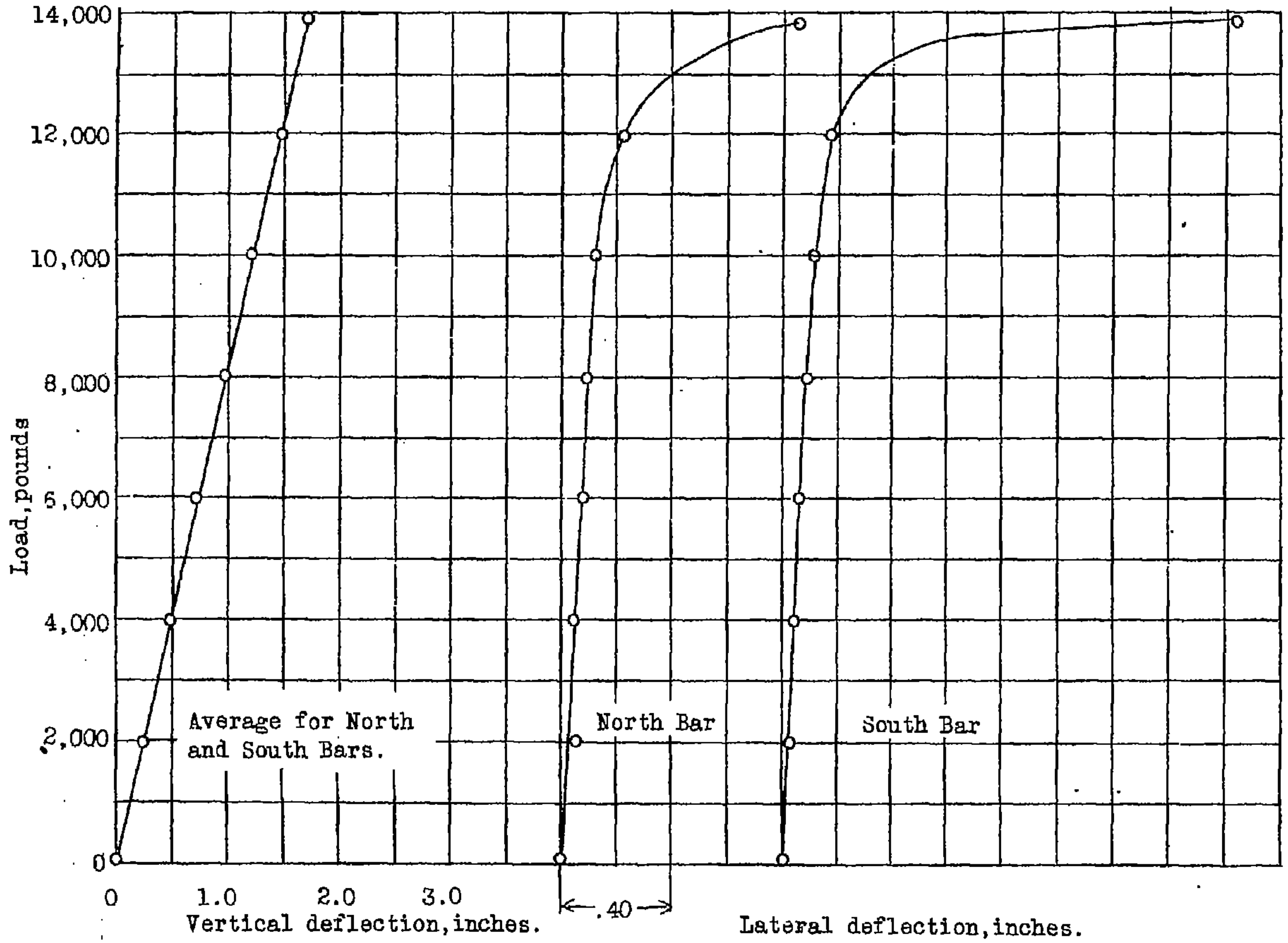


Figure 5.- Load-deflection curves for rectangular bars on edge. Span length, 96 in.; unsupported length, 72 in.; width, 1/2 in.; depth, 4 in.; 17ST aluminum alloy.

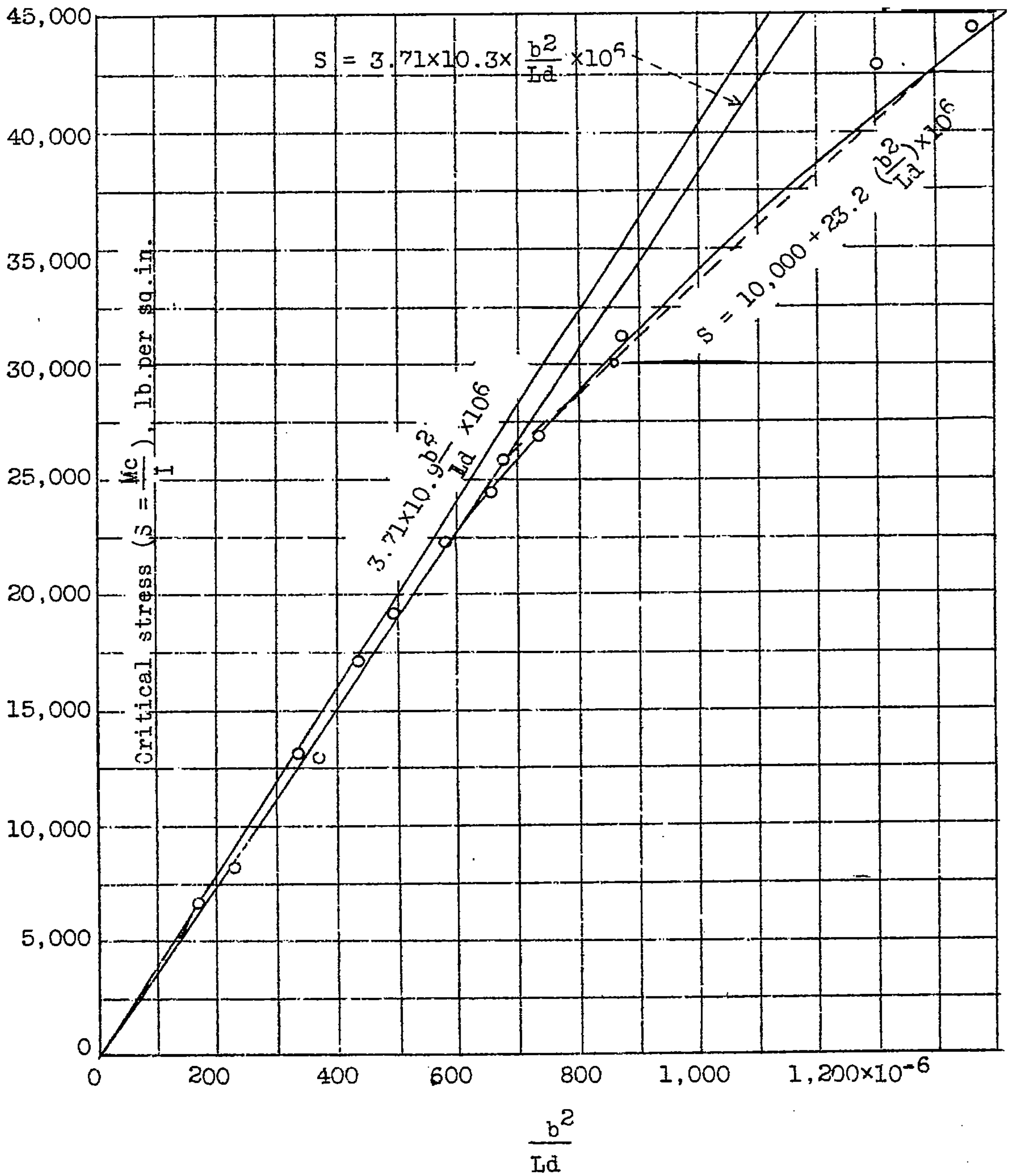


Figure 6.- Calculated and actual values for critical buckling stress for rectangular beams of 17ST aluminum alloy.

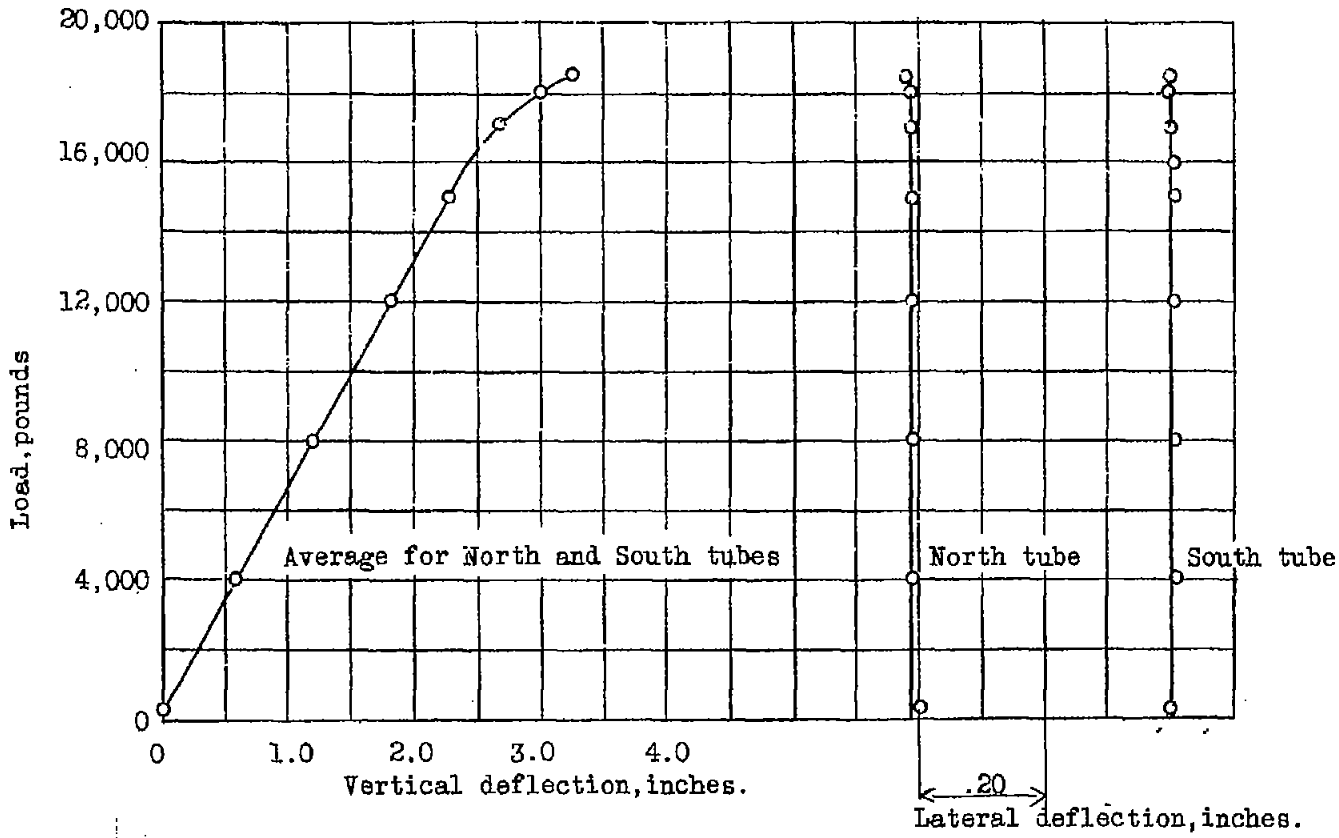


Figure 7.- Load-deflection curves for rectangular tubes on edge, $1\frac{1}{4}$"x5"x0.095" wall. Span length, 120 in.; unsupported length, 96 in.; 17ST aluminum alloy.

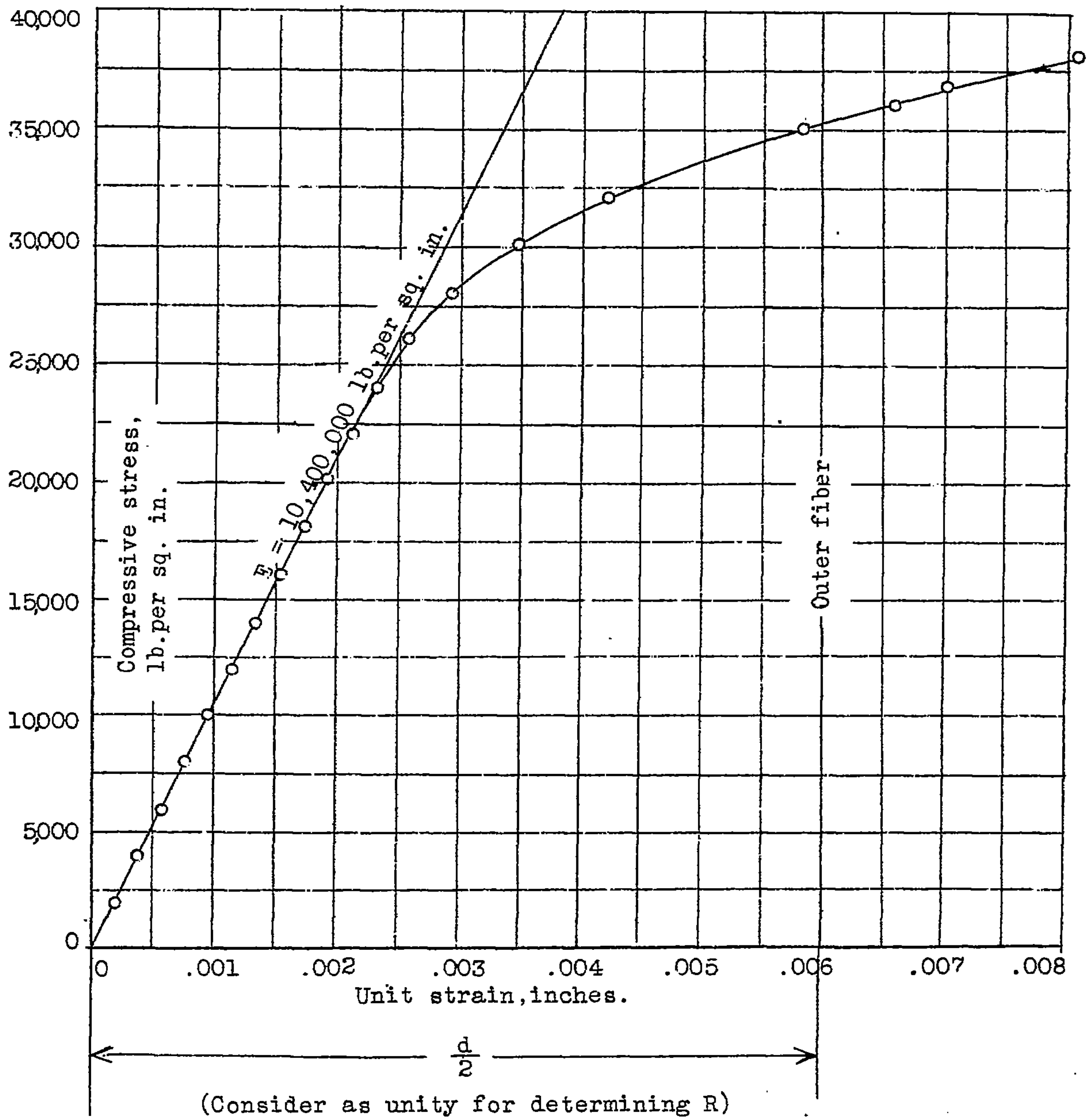


Figure 8.- Average compressive stress-strain curve for rectangular bars, 17ST aluminum alloy.

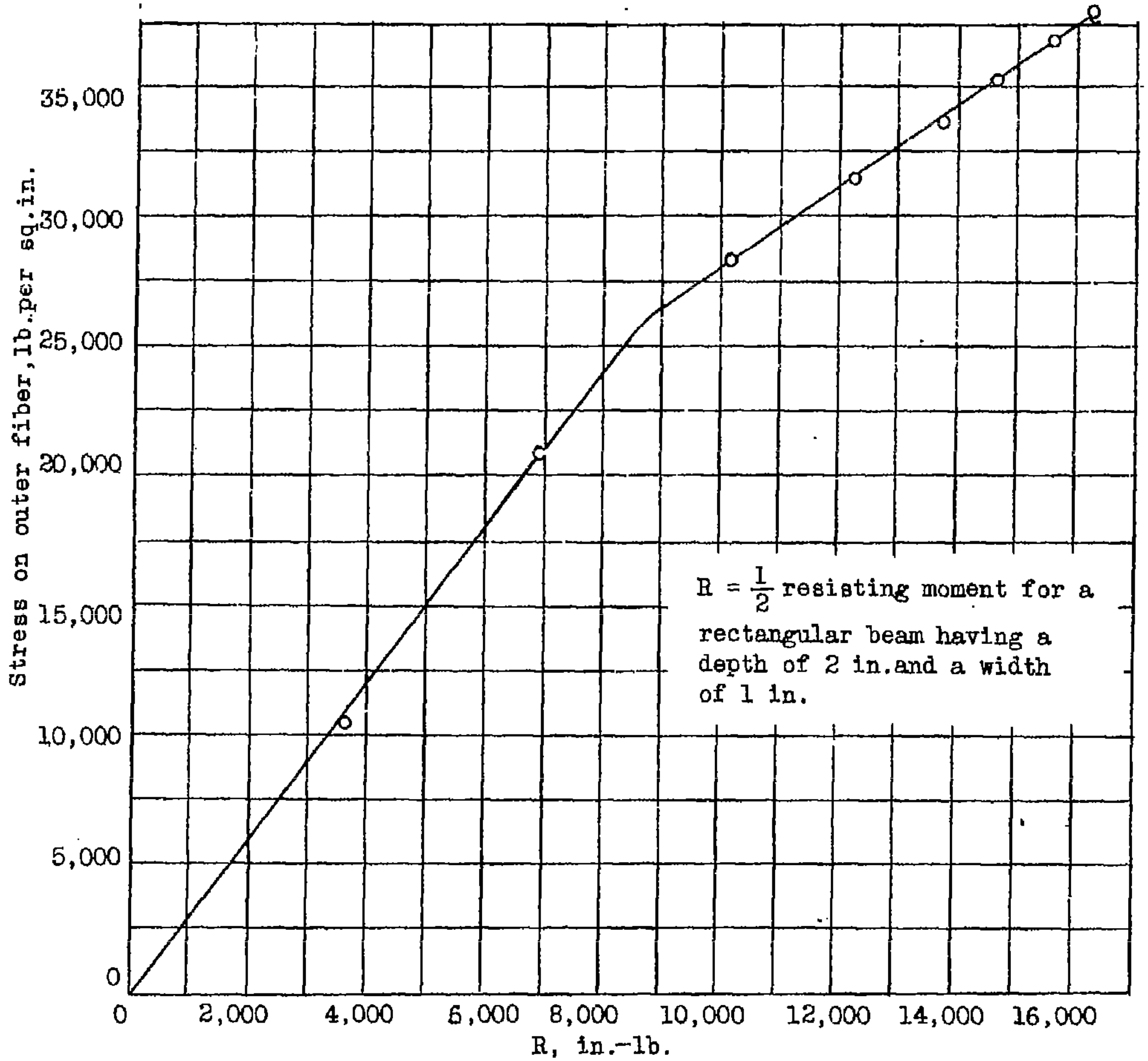


Figure 9.- Relation between true stress and factor R for rectangular beams; 17ST aluminum alloy.

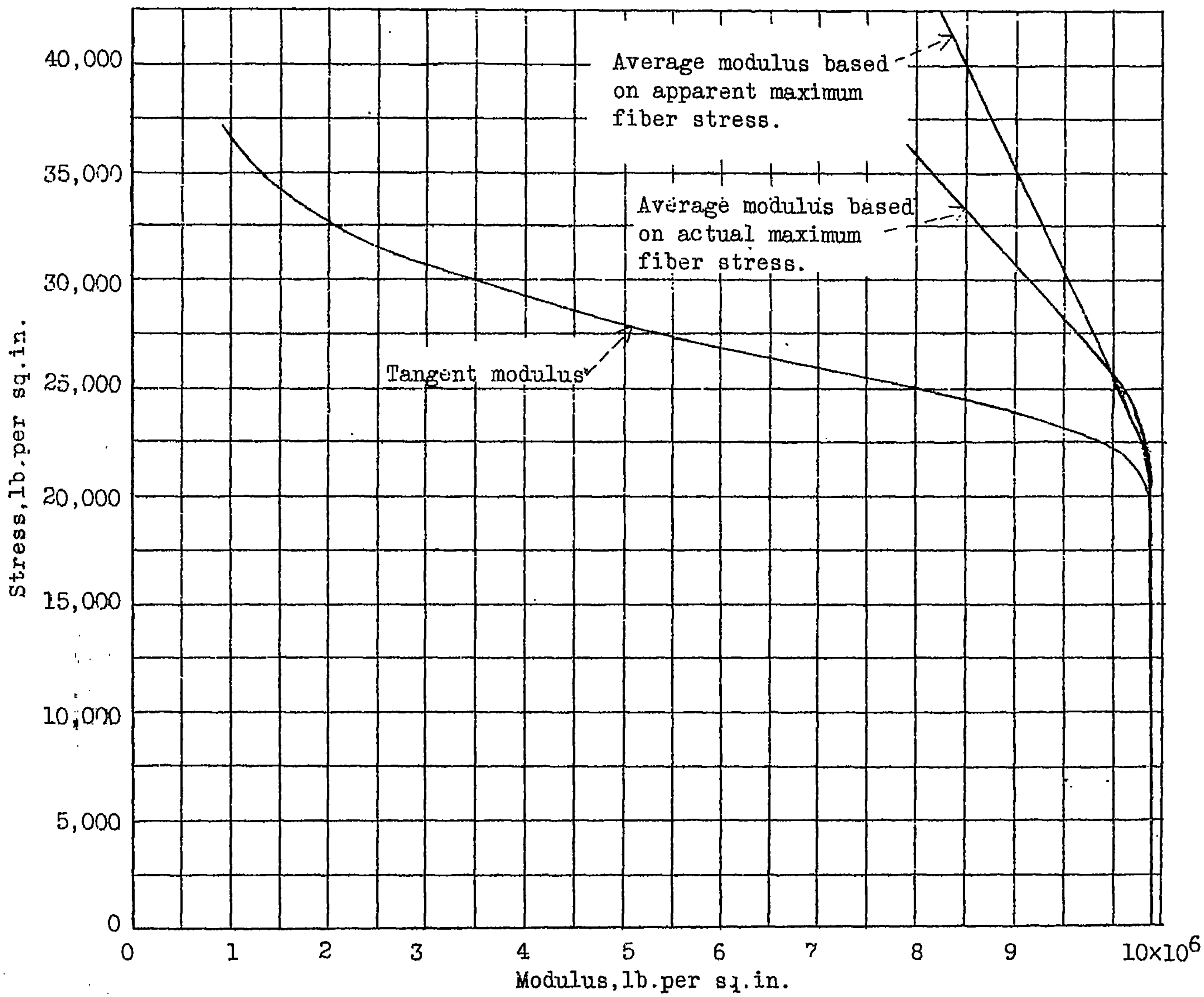


Figure 10.- Stress modulus curves for rectangular bars; 17ST aluminum alloy.

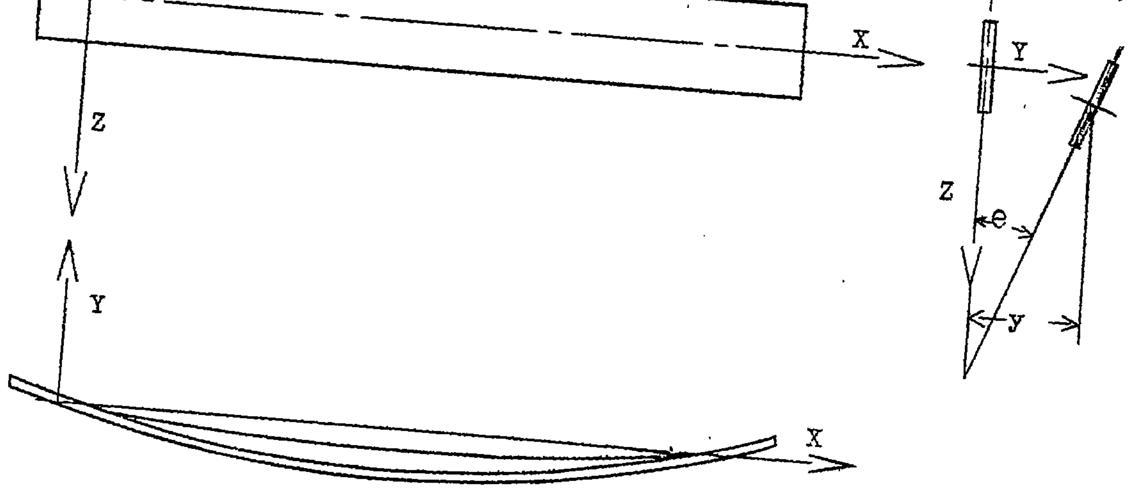


Figure 11.

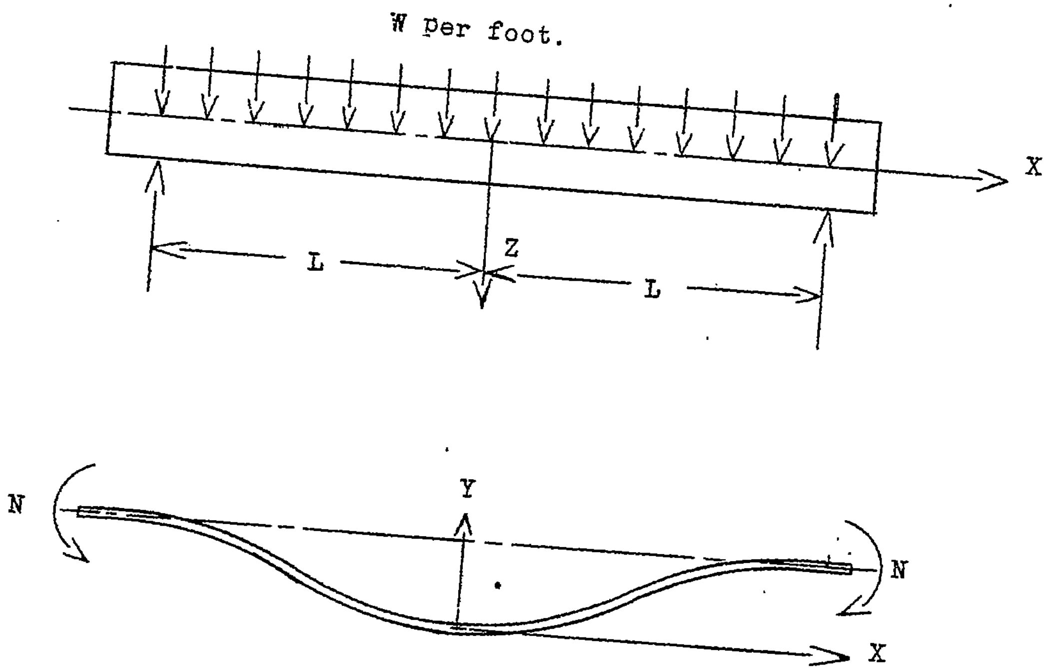


Figure 12.